

Keller's Theorem Revisited

Guillermo P. Ortiz¹ and W. Luis Mochán²

¹Departamento de Física,
Facultad de Ciencias Exactas Naturales y Agrimensura,
Universidad Nacional del Nordeste, Corrientes, Argentina
gortiz@unne.edu.ar

²Instituto de Ciencias Físicas,
Universidad Nacional Autónoma de México,
Apartado Postal 48-3, 62251 Cuernavaca, Morelos, México
mochan@fis.unam.mx

Abstract. Keller's theorem relates the components of the macroscopic dielectric response of a binary two-dimensional composite system with those of the reciprocal system obtained by interchanging its components. We present a derivation of the theorem that, unlike previous ones, does not employ the common assumption that the response function relates an irrotational to a solenoidal field and that is valid for dispersive and dissipative anisotropic systems. We show that the usual statement of Keller's theorem in terms of the conductivity is strictly valid only at zero frequency. We verify the theorem numerically in several ordered and disordered systems and discuss some of its consequences.

1. Introduction

In 1964, J. B. Keller [1] showed that for binary periodic composites made of particles in the shape of generalized cylinders with arbitrary cross sections but with certain mirror symmetries arranged in a 2D rectangular lattice within a host, the macroscopic conductivity along a principal direction is proportional to the inverse of the conductivity along the orthogonal direction of the reciprocal system, obtained from the original system by interchanging its constituent materials. The proportionality constant is the product of the conductivities of both materials. This result, known as Keller's theorem, was originally obtained by averaging the microscopic current along an edge of the unit cell [1] and writing it in terms of the electric potential, which is a solution of Laplace's equation.

The conditions under which Keller's result applies were later generalized, special cases were discussed and some applications have been developed. Keller [1] showed that for a checkerboard geometry one could obtain a simple analytical formula for the macroscopic conductivity as a simple consequence of his theorem: the macroscopic response is given simply by the geometrical mean of the conductivities of its two phases. The same formula was then shown to apply to the conductivity of a macroscopically homogeneous and isotropic but microscopically disordered 2D system made up of two phases with the same total area [2]. From this formulae, approximate [3] results for the conductivity of a 2D lattice of parallelograms and of 3D parallelepipeds for systems with high contrast have been found. Similar closed formulae have been proposed [4] and proved [5] for 2D checkerboard with more than two phases.

On the other hand, Keller's theorem has been generalized [6] to anisotropic 2D composites and a relation has been found relating the tensors that describe the macroscopic anisotropic response of a system to those of its reciprocal, in which the microscopic responses are not only interchanged but also rotated by a right angle. As a special case, the relation between the principal conductivities of systems with isotropic components but anisotropic macroscopic response were obtained [6].

Schulgasser [7] argued that a theorem analogous to Keller's theorem, in which there is a unique correspondence between the response of a system and that of its reciprocal system cannot hold in 3D. He further provided a counterexample consisting of an isotropic polycrystalline system built from a disordered mixture of randomly oriented anisotropic binary layered crystallites. Molyneux [8] has shown that for a disordered homogeneous 3D system with components described by positive definite tensors characterized by a stochastic functions with given one-, two- and three-point correlation functions one can establish strict bounds on the effective permittivity but they cannot be improved on by incorporating further correlations. For isotropic biphasic tridimensional system it has been shown that the product of the principal values of the macroscopic conductivity is bounded from below by the product of the microscopic conductivities of the constitutive phases [7, 9].

Keller's theorem can be adapted to all kinds of problems described by similar

equations. Though first derived for the electrical conductivity, it also applies to the dielectric permittivity or the thermal conductivity [10]. A recurring theme present in the derivations of Keller's theorem is that a system is excited by an irrotational field, such as an electrostatic field, or a thermal gradient, and the system responds by establishing a solenoidal field, such as an electric current, a displacement field or a heat flux. Then, use is made of the fact that a $\pi/2$ rotation interchanges the irrotational and solenoidal character of a field in 2D, so that a rotated excitation (response) may be interpreted as the response (excitation) for the reciprocal system. Thus, a question that naturally arises concerns the possible generalization of Keller's theorem to situations in which the excitation and response fields can have a different nature. For instance, the displacement field is solenoidal in the absence of external charge, but Keller's theorem might be applicable even in the presence of external charge. Similarly, an electric current is necessarily solenoidal only in the stationary case, but it is not so in the dynamical case, when excited by a time varying field.

The homogenization problem of a composite excited by oscillating sources has been analyzed by Wellander using the notion of two-scale convergence [11] for systems that occupy a finite region and when the sources of the excitation lie on its outside. Guenneau et. al. also generalized Keller's theorem to finite frequency [12]. An important physical limitation of the finite frequency generalizations is the usual assumption that the system is characterized by Hermitian response operators, thus excluding absorbing media [12]. Some other approaches for the homogenization of Maxwell equations have been proposed [13, 14, 15, 16]. In 1985 Mochán and Barrera developed a general homogenization theory in term of projection operators that allow accounting for the effects of the fluctuations of the microscopic electromagnetic fields in the the macroscopic electromagnetic response [17]. They also developed several applications of that homogenization formalism to diverse systems such as liquids, bulk crystals, crystalline surfaces and rough surfaces [18]. In this work we apply this formalism to extend Keller's theorem to the dielectric response of a 2D binary composite in the finite frequency case, allowing for dispersion and absorption, though we remain in the non-retarded regime, where the wavelength of light is assumed to be much larger than the lengthscale corresponding to the microscopic texture of the material.

The paper is organized as follows: In section 2 we obtain Keller's theorem for the dielectric tensor of 2D binary composites and study some special cases, such as isotropic systems and systems symmetric under interchange of materials. We also obtain a finite frequency generalization of Keller's theorem for the electrical conductivity. In section 3 we develop some applications of the theory. Namely, we show that the normal and parallel response functions of a superlattice are determined one from the other; we test the compliance of effective medium theories to Keller's condition; we test the accuracy of an efficient computational scheme based on Haydock's recursive method calculation [19, 20, 21] for the calculation of the macroscopic response of periodic systems; we discuss the relation among the dielectric resonances of a system and that of its reciprocal system and we explore the corresponding microscopic fields[22]; we test the accuracy of

numerical computations for ensemble members of disordered systems; and we illustrate how Keller's theorem may be used to increase the accuracy of rough approximate theories. Finally, section 4 is devoted to conclusions. In an appendix we generalize our results for the case of a composite made of anisotropic components.

2. Theory

Within a composite medium the electromagnetic fields have spatial variations due to the finite wavelength of light. They also have spatial variations due to the texture of the system. The macroscopic field has only the former variations and we will treat the latter as spatial fluctuations which we proceed to eliminate to obtain the macroscopic response $\hat{\epsilon}_M$ of the system from its *microscopic* response $\hat{\epsilon}$. The microscopic dielectric response $\hat{\epsilon}$ of a composite media is in general a linear operator which acting on the microscopic electric field \vec{E} yields the displacement field

$$\vec{D} = \hat{\epsilon}\vec{E}, \quad (1)$$

and it can be written as

$$\hat{\epsilon} = \begin{pmatrix} \hat{\epsilon}_{aa} & \hat{\epsilon}_{af} \\ \hat{\epsilon}_{fa} & \hat{\epsilon}_{ff} \end{pmatrix}, \quad (2)$$

where we define

$$\hat{\epsilon}_{\alpha\beta} \equiv \hat{\mathcal{P}}_\alpha \hat{\epsilon} \hat{\mathcal{P}}_\beta, \quad \alpha, \beta = a, f, \quad (3)$$

with $\hat{\mathcal{P}}_\alpha$ the average ($\alpha = a$) and the fluctuation ($\alpha = f$) projectors, defined such that for any field ϕ , $\phi_a \equiv \hat{\mathcal{P}}_a \phi$ is its average and $\phi_f = \hat{\mathcal{P}}_f \phi$ its fluctuations around the average, so that Eq. (1) becomes

$$\vec{D}_a = \hat{\epsilon}_{aa} \vec{E}_a + \hat{\epsilon}_{af} \vec{E}_f, \quad (4)$$

$$\vec{D}_f = \hat{\epsilon}_{fa} \vec{E}_a + \hat{\epsilon}_{ff} \vec{E}_f. \quad (5)$$

We will not pursue at this point a specific definition of what we mean by average and by fluctuation, but we demand that the corresponding operators $\hat{\mathcal{P}}_\alpha$ are projectors into complementary subspaces, that is, they should be idempotent, $\hat{\mathcal{P}}_\alpha^2 = \hat{\mathcal{P}}_\alpha$ ($\alpha = a, f$), their cross products should be null, $\hat{\mathcal{P}}_a \hat{\mathcal{P}}_f = \hat{\mathcal{P}}_f \hat{\mathcal{P}}_a = 0$ and $\hat{\mathcal{P}}_a + \hat{\mathcal{P}}_f = \hat{1}$ with $\hat{1}$ the identity operator. This means that $\hat{\mathcal{P}}_a$ throws the fluctuations away, so a second application leaves the result unchanged, $\hat{\mathcal{P}}_f$ throws the average away, so that a second application leaves the result unchanged, and throwing away the fluctuations of a field from which the average has been eliminated leaves nothing. We will also assume that these operators are space- and time-invariant, so that they commute with spatial and temporal derivatives.

Assume we excite the system with *external* charges and currents described by the densities ρ and \vec{j} that have no fluctuations, $\rho = \rho_a$, $\vec{j} = \vec{j}_a$, $\rho_f = 0$, and $\vec{j}_f = 0$. We may assume this conditions as, being external sources, ρ and \vec{j} are unrelated to the texture of

the composite. From Maxwell equations for monochromatic fields with frequency $\omega = qc$ within non-magnetic media we obtain a wave equation for the fluctuating electric field

$$\frac{1}{q^2} \nabla \times \nabla \times \vec{E}_f = \vec{D}_f = \hat{\epsilon}_{fa} \vec{E}_a + \hat{\epsilon}_{ff} \vec{E}_f, \quad (6)$$

which we formally solve for \vec{E}_f

$$\vec{E}_f = - \left(\left(\hat{\epsilon} + \frac{\nabla^2}{q^2} \hat{\mathcal{P}}^T \right)_{ff} \right)^{-1} \hat{\epsilon}_{fa} \vec{E}_a, \quad (7)$$

where we replaced $\nabla \times \nabla \times \rightarrow -\nabla^2 \hat{\mathcal{P}}^T$ and, using Helmholtz theorem, we introduced the transverse projector $\hat{\mathcal{P}}^T$ and its complement, the longitudinal projector $\hat{\mathcal{P}}^L$, so that for any vector field \vec{F} , $\vec{F}^T \equiv \hat{\mathcal{P}}^T \vec{F}$ and $\vec{F}^L \equiv \hat{\mathcal{P}}^L \vec{F}$ are its transverse and longitudinal projections, obeying $\vec{F} = \vec{F}^T + \vec{F}^L$, $\nabla \times \vec{F}^T = \nabla \times \vec{F}$, $\nabla \cdot \vec{F}^L = \nabla \cdot \vec{F}$, $\nabla \cdot \vec{F}^T = 0$, and $\nabla \times \vec{F}^L = 0$. As expected, $(\hat{\mathcal{P}}^\gamma)^2 = \hat{\mathcal{P}}^\gamma$ ($\gamma = L, T$), $\hat{\mathcal{P}}^L \hat{\mathcal{P}}^T = \hat{\mathcal{P}}^T \hat{\mathcal{P}}^L = 0$, and $\hat{\mathcal{P}}^T + \hat{\mathcal{P}}^L = \hat{1}$. In Eq. (7) we denote by $((\dots)_{ff})^{-1}$ the inverse of the operator (\dots) after having restricted it to fluctuating fields. Substituting Eq. (7) into (4) we obtain

$$\vec{D}_a = \left(\hat{\epsilon}_{aa} - \hat{\epsilon}_{af} \left(\left(\hat{\epsilon} + \frac{\nabla^2}{q^2} \hat{\mathcal{P}}^T \right)_{ff} \right)^{-1} \hat{\epsilon}_{fa} \right) \vec{E}_a = \hat{\epsilon}_M \vec{E}_a, \quad (8)$$

where we identified the macroscopic dielectric response

$$\hat{\epsilon}_M = \hat{\epsilon}_{aa} - \hat{\epsilon}_{af} \left(\left(\hat{\epsilon} + \frac{\nabla^2}{q^2} \hat{\mathcal{P}}^T \right)_{ff} \right)^{-1} \hat{\epsilon}_{fa}, \quad (9)$$

as that which relates the average displacement to the average electric field.

In analogy to Eqs. (4) and (5), we write

$$\vec{E}_a = \hat{\epsilon}_{aa}^{-1} \vec{D}_a + \hat{\epsilon}_{af}^{-1} \vec{D}_f, \quad (10)$$

$$\vec{E}_f = \hat{\epsilon}_{fa}^{-1} \vec{D}_a + \hat{\epsilon}_{ff}^{-1} \vec{D}_f, \quad (11)$$

where $\hat{\epsilon}^{-1}$ is the inverse dielectric operator. From Maxwell equations we obtain a wave equation for the fluctuating displacement field

$$\nabla^2 \hat{\mathcal{P}}^T (\hat{\epsilon}_{ff}^{-1} \vec{D}_f + \hat{\epsilon}_{fa}^{-1} \vec{D}_a) = -q^2 \hat{\mathcal{P}}^T \vec{D}_f, \quad (12)$$

where we used the absence of fluctuating external charges $\rho_f = 0$. We solve this equation for \vec{D}_f as

$$\vec{D}_f = - \left((\hat{\epsilon}^{-1} + q^2 \nabla^{-2})_{ff}^{TT} \right)^{-1} \hat{\epsilon}_{fa}^{-1} \vec{D}_a, \quad (13)$$

where we denote by $((\dots)_{ff}^{TT})^{-1}$ the inverse of the operator (\dots) after restricting it to fluctuating transverse fields. Here we introduced the inverse Laplacian ∇^{-2} as a way to denote the Green's operator $\nabla^{-2} = \hat{G}$ for Poisson's equation, $\nabla^2 \hat{G} = \hat{1}$. Substituting Eq. (13) into (10) we obtain

$$\vec{E}_a = \left(\hat{\epsilon}_{aa}^{-1} - \hat{\epsilon}_{af}^{-1} \left((\hat{\epsilon}^{-1} + q^2 \nabla^{-2})_{ff}^{TT} \right)^{-1} \hat{\epsilon}_{fa}^{-1} \right) \vec{D}_a = \hat{\epsilon}_M^{-1} \vec{D}_a, \quad (14)$$

where we identified the macroscopic inverse dielectric response

$$\hat{\epsilon}_M^{-1} = \hat{\epsilon}_{aa}^{-1} - \hat{\epsilon}_{af}^{-1} \left((\hat{\epsilon}^{-1} + q^2 \nabla^{-2})_{ff}^{TT} \right)^{-1} \hat{\epsilon}_{fa}^{-1}. \quad (15)$$

Up to this point, our results (9) and (15) are completely general, as we have introduced no approximation in their derivation. Now we will consider the long-wavelength approximation, in which we assume that the wavelength λ of a freely propagating wave of frequency ω is much larger than the lengthscale ℓ that corresponds to the texture of the composite, $\lambda \gg \ell$. We expect that ∇^2 acting on a fluctuating field to be of order $1/\ell^2$. Thus, it may safely be assumed that $\hat{\epsilon}$ is negligible compared to ∇^2/q^2 in Eq. (9) except very close to a resonance or for metallic media at frequencies where the penetration depth is close to its minimum. However, ∇^2/q^2 appears multiplied by $\hat{\mathcal{P}}^T$, so its effect is null when acting on longitudinal fields. Thus, we may approximate Eq. (9) by

$$\hat{\epsilon}_M = \hat{\epsilon}_{aa} - \hat{\epsilon}_{af} (\hat{\epsilon}_{ff}^{LL})^{-1} \hat{\epsilon}_{fa}. \quad (16)$$

Similarly, we may neglect $q^2 \nabla^{-2}$ acting on fluctuating fields when compared with ϵ^{-1} in Eq. (15) and approximate it by

$$\hat{\epsilon}_M^{-1} = \hat{\epsilon}_{aa}^{-1} - \hat{\epsilon}_{af}^{-1} \left((\hat{\epsilon}^{-1})_{ff}^{TT} \right)^{-1} \hat{\epsilon}_{fa}^{-1}. \quad (17)$$

Finally, we take the longitudinal projection of Eq. (16) and the transverse projection of Eq. (17), and we employ the block matrix theorem to obtain

$$(\hat{\epsilon}_M^{LL})^{-1} = ((\hat{\epsilon}^{LL})^{-1})_{aa} \quad (18)$$

and

$$((\hat{\epsilon}_M^{-1})^{TT})^{-1} = (((\hat{\epsilon}^{-1})^{TT})^{-1})_{aa}. \quad (19)$$

These are the main results of ref. [17].

Consider now the specific form for the transverse and longitudinal projectors,

$$\hat{P}^L = \nabla \nabla^{-2} \nabla. \quad (20)$$

and

$$\hat{P}^T = -\nabla \times \nabla^{-2} \nabla \times, \quad (21)$$

so that for any vector field \vec{F} we have

$$\vec{F}^L = \nabla \nabla^{-2} \nabla \cdot \vec{F}, \quad (22)$$

$$\vec{F}^T = -\nabla \times \nabla^{-2} \nabla \times \vec{F}, \quad (23)$$

In the particular case of 2 dimensions (2D), for fields along the $X - Y$ plane depending only on x and y , we can rewrite Eq. (23) as

$$\vec{F}^T = \nabla_R \nabla^{-2} \nabla_R \cdot \vec{F}, \quad (24)$$

where we represent ∇ as the two dimensional vector operator $(\partial/\partial_x, \partial/\partial_y)$, and ∇_R is the same operator after a 90° rotation

$$\nabla_R = \left(\frac{\partial}{\partial y}, -\frac{\partial}{\partial x} \right) = \mathbf{R} \cdot \nabla, \quad (25)$$

with

$$\mathbf{R} = \begin{pmatrix} 0 & 1 \\ -1 & 0 \end{pmatrix} \quad (26)$$

the rotation matrix, which coincides with the 2D Levy-Civita antisymmetric tensor. To avoid ambiguities in our notation and to eliminate the need for the dot products above, we represent vectors as column matrices and rewrite Eqs. (22) and (24) as matrix products,

$$\vec{F}^L = \nabla \nabla^{-2} \nabla^t \vec{F}, \quad (27)$$

and

$$\vec{F}^T = \nabla_R \nabla^{-2} \nabla_R^t \vec{F}, \quad (28)$$

with the superscript t denoting transpose.

We consider now a binary composite system made up of two isotropic local materials A , B , with corresponding dielectric functions ϵ_A and ϵ_B , so that

$$\epsilon(\vec{r}) = \epsilon_A(1 - B(\vec{r})) + \epsilon_B B(\vec{r}), \quad (29)$$

where $B(\vec{r}) = 0, 1$ is the characteristic function which takes the value 1 (0) in the regions occupied by material B (A). Notice that

$$\epsilon^{-1}(\vec{r}) = \frac{\tilde{\epsilon}(\vec{r})}{\epsilon_A \epsilon_B}, \quad (30)$$

where

$$\tilde{\epsilon}(\vec{r}) = \epsilon_B(1 - B(\vec{r})) + \epsilon_A B(\vec{r}) \quad (31)$$

corresponds to the same composite as $\epsilon(\vec{r})$ but with material A interchanged with material B . Thus, we write Eq. (19) as

$$((\hat{\epsilon}_M^{-1})^{TT})^{-1} = \epsilon_A \epsilon_B ((\hat{\epsilon}^{TT})^{-1})_{aa} \quad (32)$$

$$= \epsilon_A \epsilon_B ((\nabla_R \nabla^{-2} \nabla_R^t \hat{\epsilon} \nabla_R \nabla^{-2} \nabla_R^t)^{-1})_{aa} \quad (33)$$

$$= \epsilon_A \epsilon_B ((\mathbf{R} \nabla \nabla^{-2} \nabla^t \mathbf{R}^t \hat{\epsilon} \mathbf{R} \nabla \nabla^{-2} \nabla^t \mathbf{R}^t)^{-1})_{aa}, \quad (34)$$

where we employed the transverse projector (Eq. (24)) and introduced explicitly the rotation matrix \mathbf{R} and its transpose \mathbf{R}^t . As we assumed the microscopic response $\tilde{\epsilon}(\vec{r})$ is isotropic at each position, we can eliminate the innermost rotation matrices and write

$$((\hat{\epsilon}_M^{-1})^{TT})^{-1} = \epsilon_A \epsilon_B ((\mathbf{R} \nabla \nabla^{-2} \nabla^t \hat{\epsilon} \nabla \nabla^{-2} \nabla^t \mathbf{R}^t)^{-1})_{aa} \quad (35)$$

$$= \epsilon_A \epsilon_B ((\mathbf{R} \hat{\epsilon}^{LL} \mathbf{R}^t)^{-1})_{aa} \quad (36)$$

$$= \epsilon_A \epsilon_B \mathbf{R} ((\hat{\epsilon}^{LL})^{-1})_{aa} \mathbf{R}^t \quad (37)$$

$$= \epsilon_A \epsilon_B \mathbf{R} (\hat{\epsilon}_M^{LL})^{-1} \mathbf{R}^t, \quad (38)$$

where we identified the longitudinal projector $\hat{\mathcal{P}}^L$ from Eq. (20) and the macroscopic dielectric function from Eq. (18). We invert both sides to obtain

$$(\hat{\epsilon}_M^{-1})^{TT} = \frac{\mathbf{R} \hat{\epsilon}_M^{LL} \mathbf{R}^t}{\epsilon_A \epsilon_B}. \quad (39)$$

Now we assume that the homogenized macroscopic system is translationally invariant, so that its electromagnetic normal modes are plane waves. Let the unit vector \hat{k} be the direction of the wavevector of any of such modes, and $\hat{k}_R = \mathbf{R} \cdot \hat{k}$ the perpendicular direction. Then, we may interpret Eq. (39) as

$$\hat{k}_R \hat{k}_R^t \epsilon_M^{-1} \hat{k}_R \hat{k}_R^t = \frac{\mathbf{R} \hat{k} \hat{k}^t \tilde{\epsilon}_M \hat{k} \hat{k}^t \mathbf{R}^t}{\epsilon_A \epsilon_B}, \quad (40)$$

where we introduced the representations $\hat{\mathcal{P}}^L \rightarrow \hat{k} \hat{k}^t$ and $\hat{\mathcal{P}}^T \rightarrow \hat{k}_R \hat{k}_R^t$ of the longitudinal and transverse projectors in reciprocal space, and we represent the dielectric operators $\hat{\epsilon}_M$ and $\tilde{\epsilon}_M$ by the dielectric tensors ϵ_M and $\tilde{\epsilon}_M$. Introducing explicitly the rotation matrices, we rewrite this equation as

$$\mathbf{R} \hat{k} \hat{k}^t \mathbf{R}^t \epsilon_M^{-1} \mathbf{R} \hat{k} \hat{k}^t \mathbf{R}^t = \frac{\mathbf{R} \hat{k} \hat{k}^t \tilde{\epsilon}_M \hat{k} \hat{k}^t \mathbf{R}^t}{\epsilon_A \epsilon_B}. \quad (41)$$

We cancel the external rotation matrices, and since this equation is obeyed for arbitrary directions \hat{k} , we also cancel the projectors $\hat{k} \hat{k}^t$ to obtain finally our main result, a version of Keller's interchange theorem

$$\epsilon_M \tilde{\epsilon}_{MR} = \epsilon_A \epsilon_B \mathbf{1}, \quad (42)$$

i.e., the macroscopic dielectric tensor of a binary composite ϵ_M multiplied by the rotated macroscopic dielectric tensor of the same system but with the two materials interchanged,

$$\tilde{\epsilon}_{MR} = \mathbf{R} \tilde{\epsilon}_M \mathbf{R}^t, \quad (43)$$

is simply given by the product of the dielectric functions of the components (times the identity tensor $\mathbf{1}$).

We remark that to obtain this result we didn't assume the absence of external charges nor currents. The response functions of the system ought to be intrinsic quantities, with no dependence on the existence of external sources. Actually, some homogenization theories require external sources in their formulation. We only assumed that the sources have no spatial fluctuations, as otherwise it wouldn't make sense to pursue a macroscopic description of the response of the system. Furthermore, we made no assumption about the frequency, except for demanding that the corresponding wavelength be large in comparison with the microscopic lengthscale corresponding to the texture of the composite. The system may be periodic or random, as we only demanded that from a macroscopic point of view it should be homogeneous. The response functions of the components ϵ_A and ϵ_B may be real positive constants, corresponding to transparent dielectrics, or complex frequency dependent functions, corresponding to dissipative, dispersive media.

Some simple consequences of Eq. (42) follow: The determinant of Eq. (42) yields

$$\det(\epsilon_M) \det(\tilde{\epsilon}_M) = \epsilon_A^2 \epsilon_B^2. \quad (44)$$

In normal axes, say X, Y , it becomes

$$\epsilon_M^{xx} \tilde{\epsilon}_M^{yy} = \epsilon_M^{yy} \tilde{\epsilon}_M^{xx} = \epsilon_A \epsilon_B. \quad (45)$$

For isotropic (within the plane) composites it yields

$$\epsilon_M \tilde{\epsilon}_M = \epsilon_A \epsilon_B, \quad (46)$$

for the corresponding scalar response functions. Finally, for the very special case of an isotropic system that is invariant under the interchange $\epsilon_A \leftrightarrow \epsilon_B$, such as a periodic checkerboard or a disordered system made by adding randomly particles of each material with the same probability, we obtain from Eq. (46) the analytical result

$$\epsilon_M = \tilde{\epsilon}_M = \sqrt{\epsilon_A \epsilon_B}. \quad (47)$$

We recall that the dielectric function ϵ_α , $\alpha = A, B$ of each phase may be written in terms of its conductivity σ_α as

$$\epsilon_\alpha = 1 + \frac{4\pi i \sigma_\alpha}{\omega}, \quad (48)$$

where we incorporate in σ_α the induced currents within the system, including polarization and conduction currents. Similarly, the macroscopic response may be written in terms of a macroscopic conductivity,

$$\epsilon_M = 1 + \frac{4\pi i \sigma_M}{\omega}. \quad (49)$$

Substitution of Eqs. (48) and (49) in (42) yields

$$\sigma_M \tilde{\sigma}_{MR} - \frac{i\omega}{4\pi} (\sigma_M + \tilde{\sigma}_{MR}) = \sigma_A \sigma_B \mathbf{1} - \frac{i\omega}{4\pi} (\sigma_A + \sigma_B) \mathbf{1}, \quad (50)$$

where we used a notation analogous to that in Eq. (43). Thus, for low frequencies we recover the usual Keller's theorem for the conductivity

$$\sigma_M \tilde{\sigma}_{MR} = \sigma_A \sigma_B \mathbf{1}, \quad (51)$$

but this equality *is not obeyed at intermediate frequencies* and at large frequencies it should be replaced by a new relation

$$\sigma_M + \tilde{\sigma}_{MR} = (\sigma_A + \sigma_B) \mathbf{1}. \quad (52)$$

We remark that Keller's theorem was originally obtained for the conductivity but assuming explicitly that the divergence $\nabla \cdot \vec{j} = 0$ of the electric current density \vec{j} is zero, and using that a $\pi/2$ rotation changes curl-free fields to divergenceless fields and viceversa. However, that derivation becomes invalid at finite frequencies, for which $\nabla \cdot \vec{j} = i\omega\rho$ which in general is not null.

3. Applications

In this section we illustrate our generalized Keller's theorem with a few applications and some numerical calculations.

3.1. One dimensional systems

Consider a 1D system made up by stacking thin layers of materials A and B along the y direction. The electric E^x parallel to the layer surfaces is continuous across the interfaces and has a slow spatial variation across an individual layer, so it is almost constant. Thus, the macroscopic response

$$\epsilon_M^{xx} = (1 - f)\epsilon_A + f\epsilon_B = \langle \epsilon \rangle \quad (53)$$

is simply the average of the response of the components, where f is the filling fraction of the b material. According to Eq. (42)

$$\frac{1}{\epsilon_M^{yy}} = \frac{\tilde{\epsilon}_M^{xx}}{\epsilon_A \epsilon_B} = \frac{(1 - f)\epsilon_B + f\epsilon_A}{\epsilon_A \epsilon_B} = \frac{1 - f}{\epsilon_A} + \frac{f}{\epsilon_B} = \left\langle \frac{1}{\epsilon} \right\rangle. \quad (54)$$

This is a well known result which may be obtained by realizing that D^y is continuous across the interfaces and slowly varying across each layer, so that the inverse dielectric function is the average of the inverse dielectric functions of the components. Nevertheless, we have shown that according to Keller's theorem the results above are not independent, but *each one is a consequence of the other*.

3.2. Effective medium theories

In 2D Maxwell-Garnett theory assumes particles in the shape of circular cylinders each of which responds to the local field, given by an external field and the fields produced by all other particles, which is assumed to be dipolar. Assuming the particles are on a square lattice or that their positions are disordered but with no correlations beyond two particle correlations, the field produced by particles within a Lorentz cylindrical cavity would be null, while the field of those particles farther away corresponds to the sum of the macroscopic field and the depolarization field of the cavity, yielding the expression[23]

$$\frac{\epsilon_M - \epsilon_A}{\epsilon_M + \epsilon_A} = f \frac{\epsilon_B - \epsilon_A}{\epsilon_B + \epsilon_A}. \quad (55)$$

This formula equates the polarizability of a cylinder made of the homogenized composite with the response ϵ_M within a host with response ϵ_A with the volume average 2D polarizability of cylinders with response ϵ_B within the host A , i.e., the polarizability weighted by the filling fraction f of material B .

Interchanging materials yields the response of the reciprocal system

$$\frac{\tilde{\epsilon}_M - \epsilon_B}{\tilde{\epsilon}_M + \epsilon_B} = f \frac{\epsilon_A - \epsilon_B}{\epsilon_A + \epsilon_B}. \quad (56)$$

As the right hand sides of equations (55) and (56) are equal but for a sign change, we may write

$$\frac{\tilde{\epsilon}_M - \epsilon_B}{\tilde{\epsilon}_M + \epsilon_B} = -\frac{\epsilon_M - \epsilon_A}{\epsilon_M + \epsilon_A}, \quad (57)$$

from which Eq. (46) follows immediately.

On the other hand, the symmetrical Bruggeman's effective medium theory doesn't differentiate between host and particles and treats both materials A and B on the same footing. It postulates that the average polarizability of particles made up of materials A and B within a host made up of the homogenized composite, weighted with the corresponding filling fractions $1 - f$ and f , should be null. For circular cylindrical particles, this is represented by the equation[23]

$$(1 - f) \frac{\epsilon_A - \epsilon_M}{\epsilon_A + \epsilon_M} + f \frac{\epsilon_B - \epsilon_M}{\epsilon_B + \epsilon_M} = 0. \quad (58)$$

We may rewrite this equation as

$$\epsilon_M = \frac{\epsilon_A \epsilon_B}{\epsilon_M} + (1 - 2f)(\epsilon_A - \epsilon_B). \quad (59)$$

When the media A and B are interchanged, this equation becomes

$$\tilde{\epsilon}_M = \frac{\epsilon_A \epsilon_B}{\tilde{\epsilon}_M} - (1 - 2f)(\epsilon_A - \epsilon_B). \quad (60)$$

Adding Eqs. (59) and (60) yields

$$\epsilon_M + \tilde{\epsilon}_M = \epsilon_A \epsilon_B \left(\frac{1}{\epsilon_M} + \frac{1}{\tilde{\epsilon}_M} \right), \quad (61)$$

from which Eq. (46) follows immediately.

3.3. Periodic system

To illustrate the use of Keller's theorem to test numerical calculations of the macroscopic dielectric response, we first consider a square array of cylindrical metallic wires in vacuum and its reciprocal system made up of a square array of cylindrical holes within a metallic host (Fig. 1). For simplicity we model the metallic phase with the Drude response

$$\epsilon_D(\omega) = 1 - \omega_p^2 / (\omega^2 + i\omega\gamma) \quad (62)$$

with a moderate damping characterized by the mean collision frequency $\gamma = 0.01\omega_p$. We calculate ϵ_M and $\tilde{\epsilon}_M$ for these systems employing an efficient procedure [24, 20, 19, 25, 26] based on Haydock's recursive method (HRM) [27] and implemented in the *Photonic* computational package [28].

In Fig. 2 we show the response $\tilde{\epsilon}^M$ of an array of holes within a metallic host with a small filling fraction $f = 0.1$, calculated with the HRM. We also show $\tilde{\epsilon}_M$ as obtained through the use of Keller's theorem from the response ϵ_M of an array of wires in vacuum, calculated with the HRM. The agreement between both calculations is very good even at the peaks. In the figure we have indicated the resonance frequency $\tilde{\omega}^{(1)} \approx 0.74\omega_p$, corresponding to a peak in $\text{Im} \tilde{\epsilon}_M$. This resonance is a dipolar resonance and is slightly blue shifted from that corresponding to the dipolar surface plasmon of a single cylindrical hole, at $\tilde{\omega}_d = \omega_p / \sqrt{2}$ due to the interaction with neighbor holes. We also indicate in the figure the zero $\omega^{(1)} \approx 0.67\omega_p$ of the real part of $\text{Re} \tilde{\epsilon}_M$, which, according to Keller's theorem, corresponds to a resonance in the response ϵ_M of an array of wires. This is

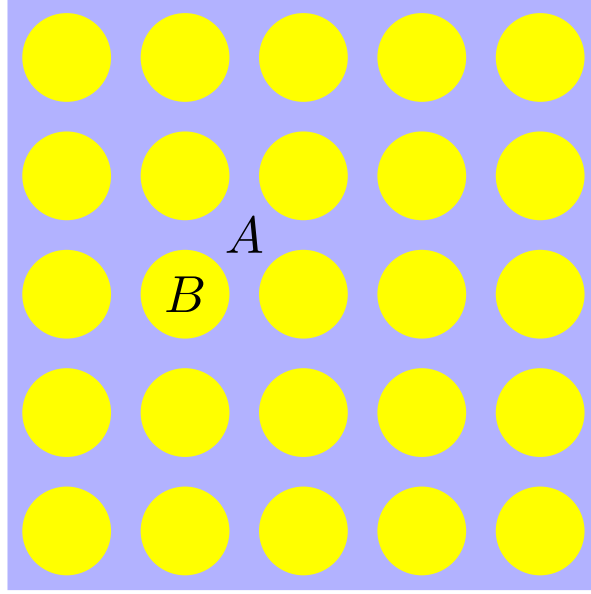


Figure 1. Cross section of a square lattice of cylindrical inclusions A with response ϵ_A within a host B of response ϵ_B .

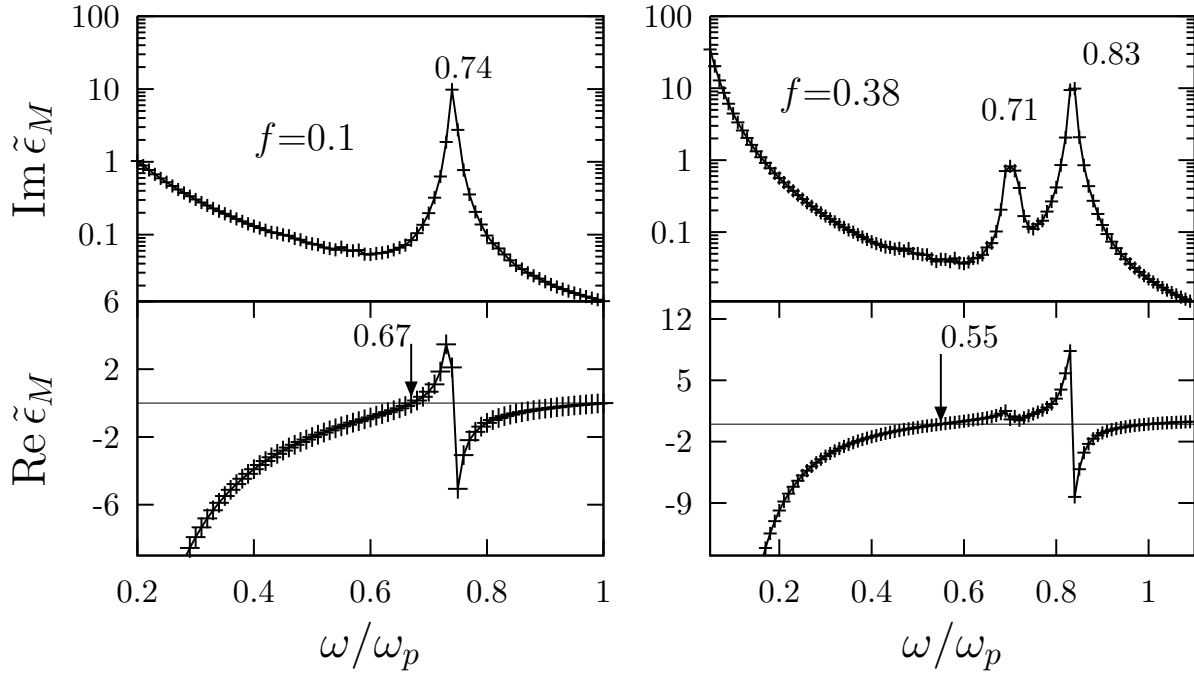


Figure 2. Real and imaginary parts of the macroscopic response $\tilde{\epsilon}_M$ of a square lattice of cylindrical holes within a Drude metal as a function of frequency for a relatively low (left panels) and an intermediate (right panel) filling fraction $f = 0.1$ and $f = 0.38$. The continuous line corresponds to the HRM numerical calculation of $\tilde{\epsilon}_M$. The crosses correspond to the use of Keller's theorem to obtain $\tilde{\epsilon}_M$ from the response ϵ_M of an array of wires in vacuum, obtained from the HRM with the same Haydock coefficients but a different spectral variable. We indicate the frequencies of the peaks of $\text{Im } \tilde{\epsilon}_M$ and the zeroes of $\text{Re } \tilde{\epsilon}_M$.

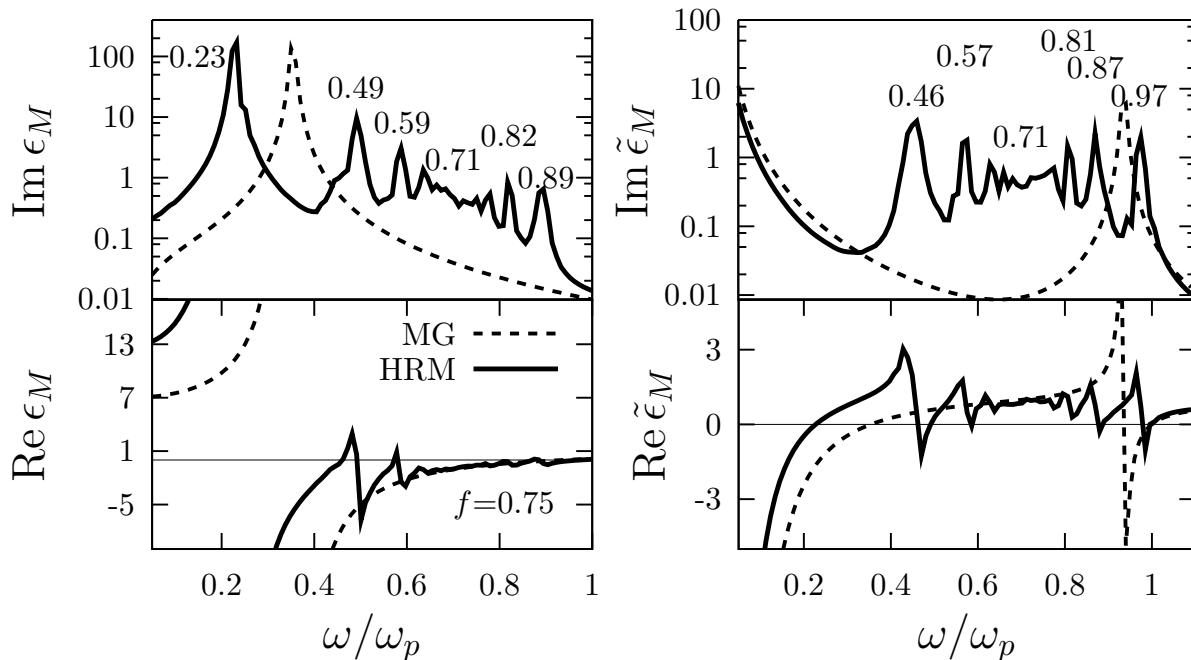


Figure 3. Real and imaginary parts of the macroscopic dielectric response of a square lattice of cylindrical wires in vacuum (right panels) and a square lattice of cylindrical holes within a metal for a high filling fraction $f = 0.75$, calculated with the HRM (solid) and with the MG approximation (dashed). The conducting phases are described by the Drude response. The frequencies of a few resonances are indicated, as well as the resonance frequency of an isolated wire or hole close to $0.71\omega_p$.

slightly red-shifted with respect to the dipolar surface plasmon $\omega_d = \omega_p/\sqrt{2} = \tilde{\omega}_d$ of a single cylindrical wire.

In Fig. 2 we also show results for a system with a higher filling fraction $f = 0.38$. The HRM calculation for a lattice of holes and the application of Keller's theorem to the HRM calculation for a lattice of wires are again in very good agreement. In this case the interactions among inclusions are stronger and the dipolar peak is further blue shifted up to $\tilde{\omega}^{(1)} \approx 0.83\omega_p$, while the zero is red shifted to $\omega^{(1)} \approx 0.55\omega_p$.

Notice that for both $f = 0.1$ and $f = 0.38$, the resonances $\omega^{(1)}$ and $\tilde{\omega}^{(1)}$ are well described by the 2D Maxwell-Garnett theory (Eqs. (55) and (56)), which for this system yield $\omega^{(1)} = \sqrt{((1-f)/2)}\omega_p$ and $\tilde{\omega}^{(1)} = \sqrt{((1+f)/2)}\omega_p$. Nevertheless, for $f = 0.38$ there is a further resonance at $\omega^l \approx 0.71\omega_p$. This is related to the excitation at large filling fractions of multipoles of higher order than the dipole. Curiously, for a cylindrical single wire and for a single hole all the multipolar resonances are degenerate with the dipolar surface plasmon at $\omega_p/\sqrt{2}$.

In Fig.3 we show ϵ^M and $\tilde{\epsilon}^M$ calculated with the HRM for the same system as in Fig. 2 but with a high filling fraction $f = 0.75$. As a reference, we also show the results of MG theory. While MG predicts a single peak with a dipolar character, the numerical HRM calculation yields several peaks with multipolar contributions, five of which are

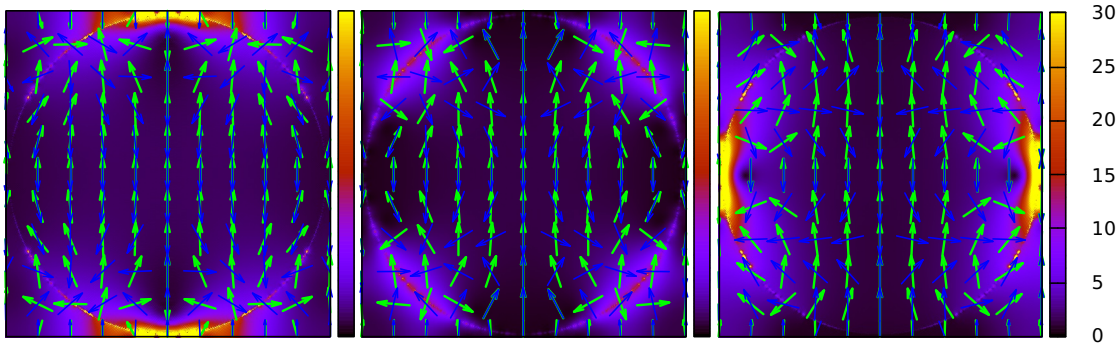


Figure 4. Direction of the real (green arrows) and imaginary (blue arrows) parts of the microscopic field and field magnitude (color map) for a square lattice of wires with a filling fraction $f = 0.75$ as in Fig. 3 excited with a homogeneous external field of unit magnitude along the vertical direction corresponding from left to right to the frequencies $\omega = 0.59\omega_p$, $\omega = 0.71\omega_p$ and $\omega = 0.82\omega_p$.

clearly visible. Of these, some are blue shifted and some are red shifted with respect to the resonant frequency of an isolated wire and an isolated hole. We expect that the peak in ϵ_M that is furthest red shifted and the peak in $\tilde{\epsilon}_M$ that is furthest blue shifted correspond to the modes with the largest dipolar contribution. Both of these shifts are close but larger than those predicted by MG theory.

The results above can be understood from the fact that within the HRM we can write

$$\epsilon_M = \epsilon_A F(u), \quad \tilde{\epsilon}_M = \epsilon_B F(\tilde{u}), \quad (63)$$

where $u = 1/(1 - \epsilon_A/\epsilon_B)$ and $\tilde{u} = 1/(1 - \epsilon_B/\epsilon_A)$ are the *spectral variables* of the system and its reciprocal system, and where F is a function given by a continued fraction determined by the *Haydock* coefficients which are determined exclusively by the geometry of the system. Notice that $\tilde{u} = 1 - u$, so that any resonance u^* in the function F corresponds to a resonance frequency ω^* in the system, such that $u(\omega^*) = u^*$, and a corresponding resonance $\tilde{\omega}^*$ in the reciprocal system, such that $\tilde{u}(\tilde{\omega}^*) = 1 - u(\tilde{\omega}^*) = u^*$. Thus, according to Keller's theorem, for each resonance ω_n in ϵ_M there must be a corresponding resonance $\tilde{\omega}_n$ in $\tilde{\epsilon}_M$ and for the Drude model, they should be related through $\omega_n^2 + \tilde{\omega}_n^2 = \omega_p^2$. From Fig. 3 we can verify that this is the case as $0.23^2 + 0.97^2 \approx 0.49^2 + 0.87^2 \approx 0.59^2 + 0.81^2 \approx 0.82^2 + 0.57^2 \approx 0.89^2 + 0.46^2 \approx 1$.

In Fig. 4 we show the microscopic electric field in a lattice of wires, as in Fig. 3 for three frequencies: the resonance at $\omega \approx 0.59\omega_p$, the dipolar plasmon frequency $\omega = \omega_p/\sqrt{2}$ of an individual wire and the resonance at $\omega = 0.82\omega_p$. The calculation was performed with the *Photonic* code[28]. Note that in the middle panel the intensity of the field is the same along the horizontal and vertical directions. In the left panel, corresponding to a resonance that has been red shifted from that of the single wire, the field is much more intense close to the surface of the wires along the vertical direction, which coincides with the direction of the external field, while in the right

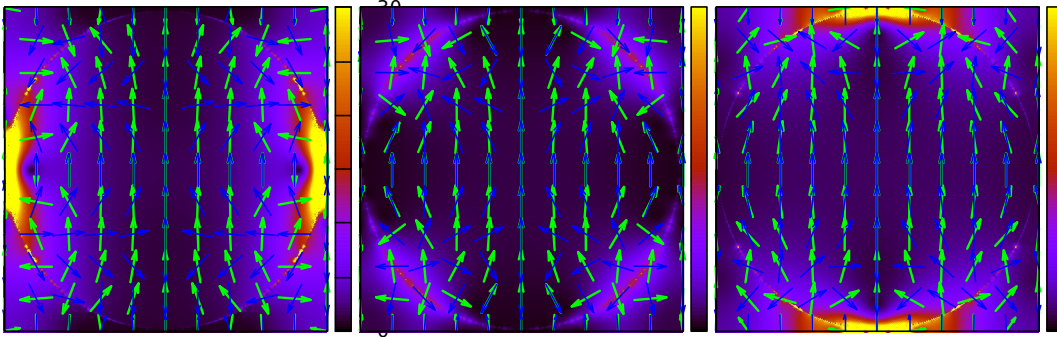


Figure 5. Direction of the real (green arrows) and imaginary (blue arrows) parts of the microscopic field and field magnitude (color map) for the system reciprocal to that of Fig. 4, i.e., a square lattice of holes within a conductor with a filling fraction $f = 0.75$ excited with a homogeneous external field of unit magnitude along the vertical direction corresponding from left to right to the frequencies $\omega = 0.57\omega_p$, $\omega = 0.71\omega_p$ and $\omega = 0.81\omega_p$.

panel, corresponding to a resonance that has been blue shifted with respect to that of an isolated wire, the intensity is higher along the horizontal direction, perpendicular to the external field. We have verified a similar behavior for the other resonances to the left and right of the isolated surface plasmon.

Fig. 5 we show the microscopic field for a lattice of holes, the reciprocal system to that in Fig. 4, for the resonance at $\tilde{\omega} = 0.57\omega_p$, the dipolar surface plasmon frequency $\tilde{\omega}^{(2)} = 0.71\omega_p$ of an isolated cylindrical hole within a Drude conductor, and $\tilde{\omega} = 0.81\omega_p$. We note that the field distribution for each panel is similar to the field distribution shown in Fig. 4 for the corresponding paired frequency ω , with $\omega^2 + \tilde{\omega}^2 = \omega_p^2$. Thus, the panels of Fig. 5 going from left to right correspond to the panels of Fig. 4 going from right to left. For frequencies smaller than that of the isolated surface plasmon the field is maximum at the surface of the holes in direction normal to the external field, while at frequencies larger than that of the isolated surface plasmon the maxima lie along the direction of the external field.

The results above (Figs. 2-5) were calculated for an isotropic material, for which the Haydock coefficients, and thus the function F of Eq. (63), are invariant under rotations. Thus the only change in going from the system of wires to the system of holes is the substitution $u \rightarrow \tilde{u} = 1 - u$. This is not the case for an anisotropic system. In Fig. 6 we show the response of an array of holes calculated with the HRM and that obtained by applying Keller's theorem to the response of the corresponding array of wires, as in Fig. 2, but for an anisotropic rectangular array with sides in a 3:2 ratio and for a high filling fraction $f = 0.5$. The direction of the field for the array of holes was taken along the short and along the long sides of the rectangular unit cell (left and right panels respectively). Note that, unlike Fig. 3, Fig. 6 shows more resonances shifted towards one side than towards the opposite side of the surface plasmon of the isolated hole. This is consistent with Fig. 5 which shows that for $\omega < \omega_p/\sqrt{2}$ the field is maximum along

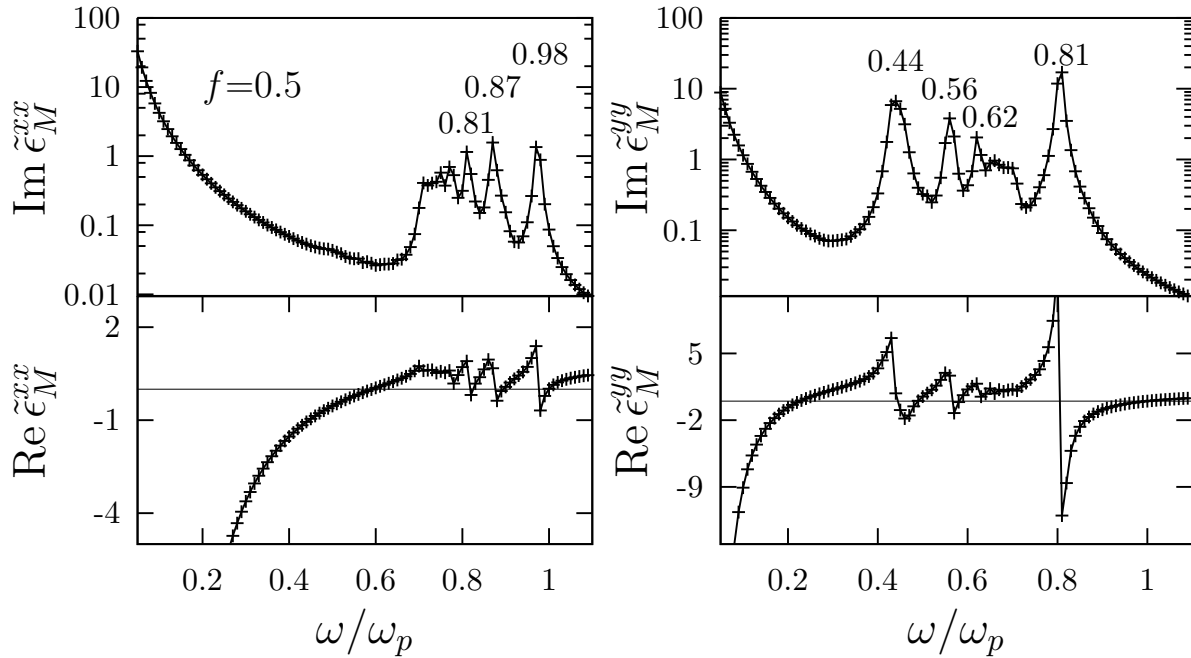


Figure 6. Real and imaginary parts of principal values of the macroscopic response of a rectangular array of cylindrical holes within a Drude conductor as a function of frequency for an aspect ratio 3:2 and for a filling fraction $f = 0.5$, calculated with the HRM (solid) and applying Keller's theorem to the response of the corresponding array of cylindrical wires (crosses). The field points either along the short side (left panel) or along the long side (right panel) of the rectangular unit cell, for the case of the array of holes, and in the perpendicular direction for the case of wires.

the direction normal to that of the external field. Thus, it points along the long side of the unit cell in the left side of the left panel of Fig. 6, producing no visible structure, and along its short side for the right panel, producing a strong interaction among the holes and thus a rich resonant structure. On the other hand, for $\omega > \omega_p/\sqrt{2}$, the field is stronger along the field's direction, and therefore, it produces strong interactions and a rich structure in the right side of the left panel of Fig. 6 and only a single blueshifted resonance in the right panel. In this case, the Haydock coefficients used for the direct calculation of the array of holes is different from those used for the array of wires, due to the $\pi/2$ rotation required by Keller's theorem. Nevertheless, the direct calculation of $\tilde{\epsilon}_M$ and the calculation using Keller's theorem are in excellent agreement.

3.4. Disordered Systems

We consider now the response of a disordered system, approximated by an ensemble of periodic systems with a large unit cell within which N wires are set at random positions, as illustrated in Fig.7. In Fig. 8 we show the components $\tilde{\epsilon}_M^{\alpha\beta}$ of the dielectric tensor calculated with the HRM for one realization of the reciprocal system, consisting of a

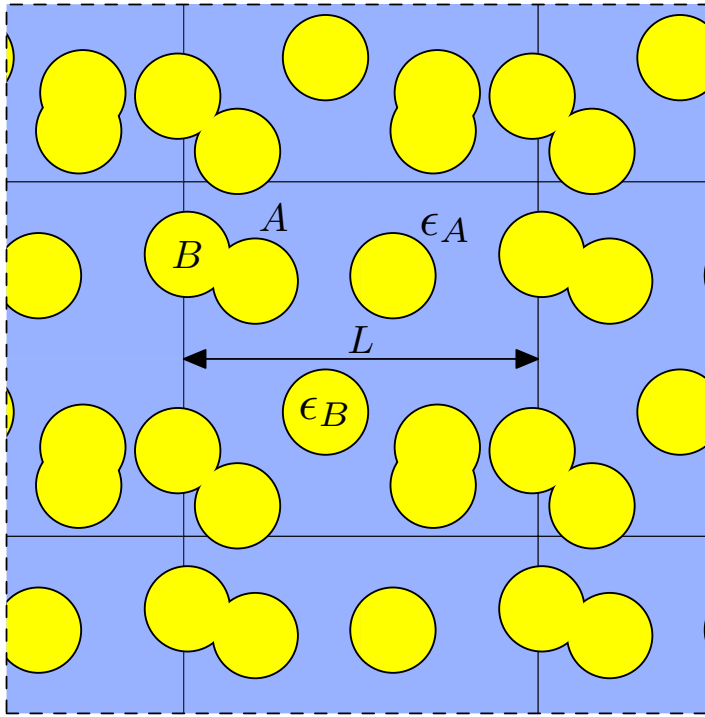


Figure 7. Illustration of a disordered system approximated by the periodic repetition of a relatively large unit cell within which numerous wires occupy random positions.

disordered array of cylindrical holes within a conductor. We took $N = 30$ holes and distributed them randomly without correlation, allowing the holes to overlap. In the same figure we show the result obtained by first calculating the response $\epsilon_M^{\alpha\beta}$ of the corresponding disordered system of conducting wires in vacuum and then using the tensorial version of Keller's theorem Eq. (42). Notice that although the disordered system is isotropic, a single member of the ensemble with a finite number of particles is anisotropic, its principal directions are not necessarily aligned with the cartesian axes and thus they may depend on frequency, so that ϵ^M is not a diagonal matrix. The response shows a very rich structure due to the strong coupling between neighbor holes, with fluctuating nearest neighbor distances and with several pairs of overlapping neighbors. Nevertheless, Keller's theorem seems to hold quite well by our HRM calculations.

To explore the fulfillment of Keller's theorem for disordered systems with different filling fractions, we have varied the radius of the wires/holes for the same ensemble member as in Fig. 8 and we evaluated the deviation from Keller's theorem

$$\Delta K = 2 \left| \frac{\det(\tilde{\epsilon}^M) \det(\epsilon^M) - \epsilon_A^2 \epsilon_B^2}{\det(\tilde{\epsilon}^M) \det(\epsilon^M) + \epsilon_A^2 \epsilon_B^2} \right|. \quad (64)$$

In Fig.9 we show ΔK as function of frequency and filling fraction f . For this calculation we used a more modest discretization of only 201×201 pixels. Nevertheless, the deviation away from Keller's theorem is very small except for a few resonances at the smallest

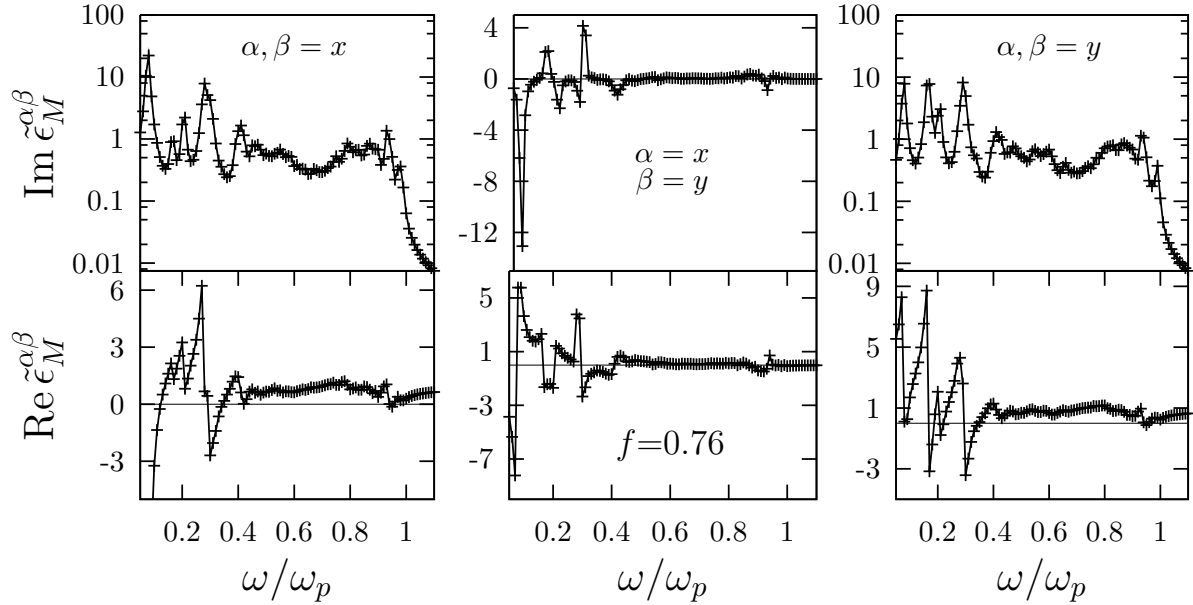


Figure 8. Frequency dependence of the real and imaginary parts of the components $\tilde{\epsilon}_M^{\alpha\beta}$ (solid) of the dielectric tensor calculated with the HRM for a single member of an ensemble that approximates a disordered system made up of cylindrical holes within a Drude conducting host as illustrated in Fig. 7. The system consists of 30 cylinders of radius $a = 0.12L$ randomly distributed without correlation among their positions within a square unit cell of side L discretized to 501×501 pixels. The filling fraction is $f = 0.76$. We also show the corresponding result obtained from the dielectric tensor of the corresponding system of conducting wires in vacuum by employing the tensorial version of Keller's theorem (Eq. 42) (crosses).

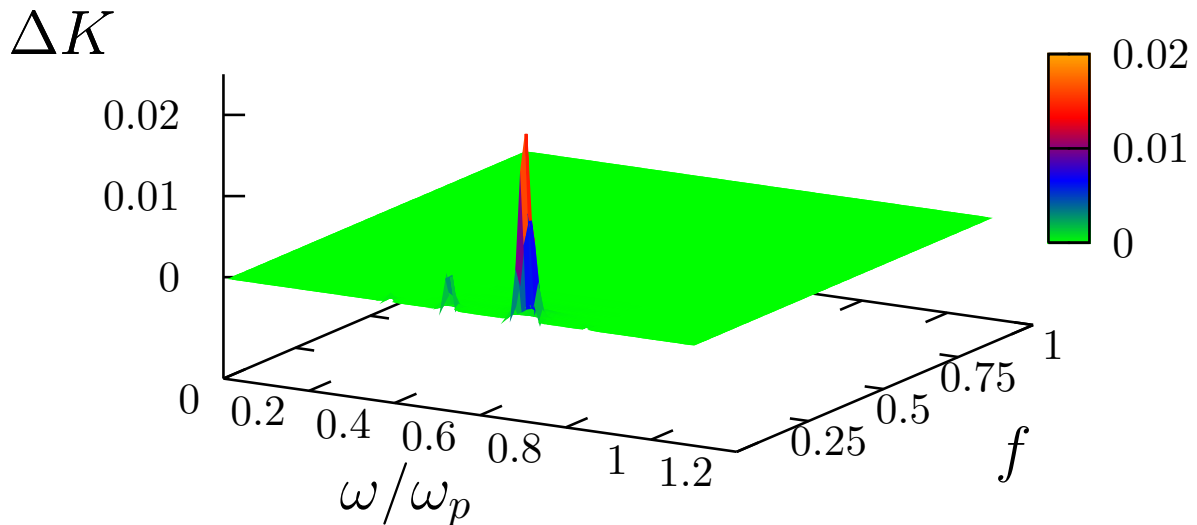


Figure 9. ΔK as function of frequency ω and filling fraction f for the same realization of the disordered system as in Fig. 8 but calculated in a unit cell of only 201×201 pixels.

filling fractions $f = 0.1$ for which the pixelated representation of the wires and holes is inadequate.

We have verified that our HRM calculations for this system also hold after averaging over a large enough ensemble.

3.5. Convergence Acceleration

Keller's theorem must hold for the *exact* nonretarded macroscopic dielectric tensors ϵ_M^E and $\tilde{\epsilon}_M^E$ of a binary 2D composite and its reciprocal system, but it may well fail for the dielectric tensors ϵ_M and $\tilde{\epsilon}_M$ obtained from an approximate numerical calculation. If we write the exact dielectric tensor of a system and its reciprocal as

$$\epsilon_M^E = \epsilon_M + \delta\epsilon_M, \quad \tilde{\epsilon}_M^E = \tilde{\epsilon}_M + \delta\tilde{\epsilon}_M, \quad (65)$$

we can write Eq.(42), as

$$(\epsilon_M + \delta\epsilon_M)\mathbf{R}(\tilde{\epsilon}_M + \delta\tilde{\epsilon}_M)\mathbf{R}^t = \epsilon_A\epsilon_B, \quad (66)$$

that linearizing in $\delta\epsilon_M$ and $\delta\tilde{\epsilon}_M$ becomes a system of four equations

$$\begin{aligned} & \begin{pmatrix} \delta\epsilon_M^{xx} & \delta\epsilon_M^{xy} \\ \delta\epsilon_M^{yx} & \delta\epsilon_M^{yy} \end{pmatrix} \begin{pmatrix} \epsilon_M^{yy} & -\epsilon_M^{yx} \\ -\epsilon_M^{xy} & \epsilon_M^{xx} \end{pmatrix} + \begin{pmatrix} \epsilon_M^{xx} & \epsilon_M^{xy} \\ \epsilon_M^{yx} & \epsilon_M^{yy} \end{pmatrix} \begin{pmatrix} \delta\epsilon_M^{yy} & -\delta\epsilon_M^{yx} \\ -\delta\epsilon_M^{xy} & \delta\epsilon_M^{xx} \end{pmatrix} = \\ & \begin{pmatrix} \epsilon_A\epsilon_B & 0 \\ 0 & \epsilon_A\epsilon_B \end{pmatrix} - \begin{pmatrix} \epsilon_M^{xx} & \epsilon_M^{xy} \\ \epsilon_M^{yx} & \epsilon_M^{yy} \end{pmatrix} \begin{pmatrix} \epsilon_M^{yy} & -\epsilon_M^{yx} \\ -\epsilon_M^{xy} & \epsilon_M^{xx} \end{pmatrix} \end{aligned} \quad (67)$$

in the six complex unknowns $\delta\epsilon_M^{xx}$, $\delta\epsilon_M^{xy} = \delta\epsilon_M^{yx}$, $\delta\epsilon_M^{yy}$, $\delta\tilde{\epsilon}_M^{xx}$, $\delta\tilde{\epsilon}_M^{xy} = \delta\tilde{\epsilon}_M^{yx}$, and $\delta\tilde{\epsilon}_M^{yy}$, which we write as the matrix equation

$$\mathbf{M}\mathbf{I} = \mathbf{D}, \quad (68)$$

where

$$\mathbf{I} = \begin{pmatrix} \delta\epsilon_M^{xx} \\ \delta\epsilon_M^{xy} \\ \delta\epsilon_M^{yy} \\ \delta\tilde{\epsilon}_M^{xx} \\ \delta\tilde{\epsilon}_M^{xy} \\ \delta\tilde{\epsilon}_M^{yy} \end{pmatrix}, \quad (69)$$

and

$$\mathbf{M} = \begin{pmatrix} \tilde{\epsilon}_M^{yy} & -\tilde{\epsilon}_M^{xy} & 0 & 0 & -\epsilon_M^{xy} & \epsilon_M^{xx} \\ -\tilde{\epsilon}_M^{yx} & \tilde{\epsilon}_M^{xx} & 0 & \epsilon_M^{xy} & -\epsilon_M^{xx} & 0 \\ 0 & -\tilde{\epsilon}_M^{yx} & \tilde{\epsilon}_M^{xx} & \epsilon_M^{yy} & -\epsilon_M^{yx} & 0 \\ 0 & \tilde{\epsilon}_M^{yy} & -\tilde{\epsilon}_M^{xy} & 0 & -\epsilon_M^{yy} & \epsilon_M^{yx} \end{pmatrix}, \quad (70)$$

and

$$\mathbf{D} = \begin{pmatrix} \epsilon_A\epsilon_B - \epsilon_M^{xx}\tilde{\epsilon}_M^{yy} + \epsilon_M^{xy}\tilde{\epsilon}_M^{xy} \\ \epsilon_M^{xx}\tilde{\epsilon}_M^{yx} - \epsilon_M^{xy}\tilde{\epsilon}_M^{xx} \\ \epsilon_M^A\epsilon_B - \epsilon_M^{yy}\tilde{\epsilon}_M^{xx} + \epsilon_M^{yx}\tilde{\epsilon}_M^{yx} \\ \epsilon_M^{yy}\tilde{\epsilon}_M^{xy} - \epsilon_M^{yx}\tilde{\epsilon}_M^{yy} \end{pmatrix}. \quad (71)$$

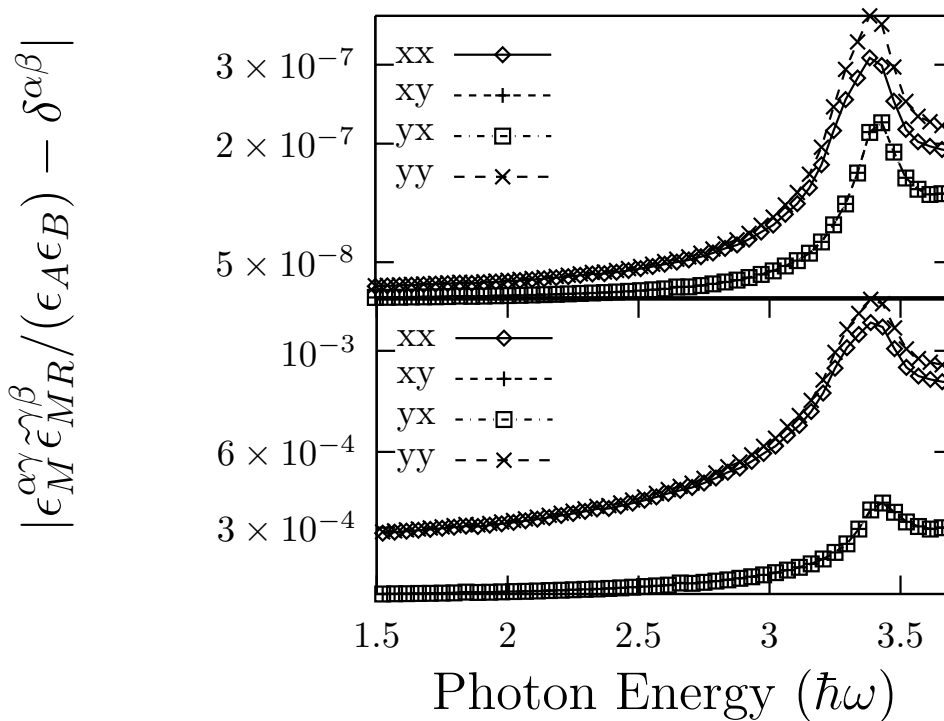


Figure 10. Absolute value of the different components of the departure of the computed dielectric tensors ϵ_M and $\tilde{\epsilon}_M$ from Keller's theorem (42) for an ensemble of one hundred realizations of a random checkerboard with ten thousand particles each consisting of Si prisms within vacuum. The bottom panel shows the result of the HRM calculation and the upper panel the result after adding corrections from Eq. (73).

Although Eq. (68) is underdetermined and doesn't have a unique solution, one may attempt to obtain the *smallest* corrections $\delta\epsilon_M$ and $\delta\tilde{\epsilon}_M$ that when added to the approximate results ϵ_M and $\tilde{\epsilon}_M$ yield response functions that better fulfill Keller's theorem and that may thus be expected to better approximate the exact results. To that end we perform a singular value decomposition (SVD) [29]

$$\mathbf{M} = \mathbf{U}\mathbf{\Sigma}\mathbf{V}^t, \quad (72)$$

where \mathbf{U} and \mathbf{V} are column-orthogonal matrices and $\mathbf{\Sigma}$ is a diagonal matrix, obtaining

$$\mathbf{I} = \mathbf{V}\mathbf{\Sigma}^{-1}\mathbf{U}^t\mathbf{D}. \quad (73)$$

To illustrate the use of Keller's theorem to improve the convergence of numerical calculations we use the HRM to make crude calculations of ϵ_M and $\tilde{\epsilon}_M$ and then correct our calculations using the procedure above get better approximations for which the deviations from Keller's condition is smaller.

In Fig. 10 we show the deviation from Keller's condition for a system made up of square Si prisms randomly occupying the sites of a square array within vacuum, with a filling fraction $f = 1/2$. We see that adding the correction (73) diminishes the deviation from Keller's condition by more than four orders of magnitude, from the order

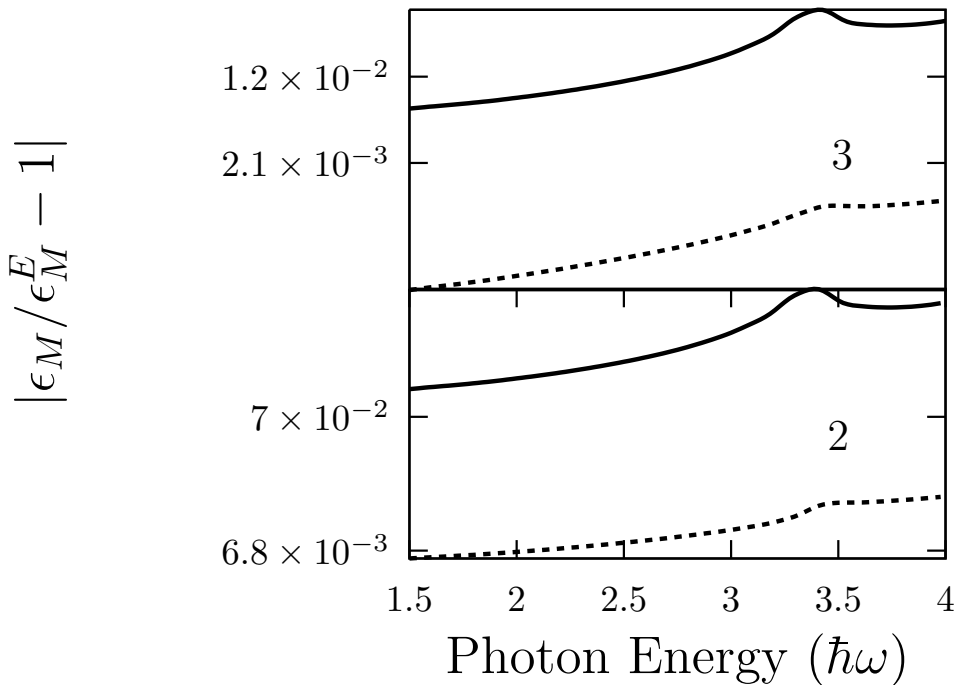


Figure 11. Relative difference between the dielectric function of ϵ_M calculated with the HRM for a square array of square Si prisms with filling fraction $f = 1/4$ within vacuum, and the exact response (74) before (solid lines) and after (dashed lines) the correction (73) is applied. The HRM calculations were performed with an extremely small number of Haydock iterations: 2 for the lower panel and 3 for the upper panel.

of 10^{-3} to 10^{-7} or better. We remark that this is an isotropic system symmetrical under the interchange of components for which the exact dielectric response is completely determined by Keller's theorem through Eq. (47).

Now we turn our attention to a system proposed by Mortola and Steffé [4] consisting of a square array of square prisms with filling fraction $f = 1/4$. It turns out that this system has the exact solution [5]

$$\epsilon_M^E = \epsilon_A \sqrt{\frac{\epsilon_A + 3\epsilon_B}{\epsilon_B + 3\epsilon_A}}. \quad (74)$$

It has been shown [30] that the HRM is capable of reproducing numerically this results, even for metallic phases. In Fig. 11 we display the relative error of the numerical calculation of the macroscopic response of a systems made up of a square lattice of square Si prisms with a filling fraction of $f=1/4$ calculated with an extremely small number of Haydock pair of coefficients $n = 2$ and $n = 3$. Not surprisingly, the crude numerical results have a large discrepancy of a few percent from the exact result. Nevertheless, an order of magnitude accuracy increase is obtained by applying the correction (73). Furthermore, better inicial results benefit from even higher accuracy increases.

4. Conclusions

We obtained a version of Keller's theorem relating the macroscopic dielectric tensor ϵ_M of 2D binary composite systems to the corresponding response $\tilde{\epsilon}_M$ of their reciprocal systems, with the same geometry but with their two components interchanged. The derivation assumes that the texture of the system has a lengthscale that is much smaller than the wavelength of light, but otherwise, is valid for finite frequencies and may be applied to dispersive and dissipative materials. We obtained results for the generic anisotropic case, and special results for the isotropic case and for systems symmetric under interchange of materials. Our results are based on a general homogenization procedure that does not require the fields to be irrotational or solenoidal, as we make no assumption about the absence of sources in the derivation. Although Keller's theorem is frequently stated in terms of the electrical conductivity σ_M , we show that in general this response only obeys Keller's theorem in the limit of very low frequencies. Nevertheless, we obtained a generalization of Keller's theorem for the conductivity at finite frequencies. We developed a few applications of Keller's theorem. Thus we showed that the expression for the response of a 1D superlattice perpendicular to its axis is determined by its response along its axis. We verified that common effective medium theories, such as Maxwell Garnett's and Bruggeman's expressions, do obey Keller's theorem. We showed how one may employ Keller's theorem to check the accuracy of numerical computations, we showed that for each resonance of an isotropic system there is a corresponding resonance of the reciprocal system described by a corresponding spectral variable and with the same microscopic field distribution. We illustrated the use of Keller's theorem to test model calculations for ordered, disordered, isotropic, and anisotropic systems. Finally, we showed that Keller's theorem may be employed to increase the accuracy of approximate numerical calculations.

Acknowledgments

We acknowledge support from DGAPA-UNAM under grant IN113016, from FONCYT under grant PICT-2013-0696, and from SGCyT-UNNE under grant PI-F008-2014.

Appendix A. Appendix: Anisotropic materials

If the materials A and B were themselves anisotropic, then instead of Eq. (29) we would have

$$\epsilon(\vec{r}) = \epsilon_A(1 - B(\vec{r})) + \epsilon_B B(\vec{r}) = \epsilon_A \mathbf{U}_A(1 - B(\vec{r})) + \epsilon_B \mathbf{U}_B B(\vec{r}), \quad (\text{A.1})$$

where $\epsilon_\alpha \equiv \epsilon_\alpha \mathbf{U}_\alpha$, ($\alpha = A, B$), $\epsilon_\alpha \equiv \sqrt{\det \epsilon_\alpha}$ and \mathbf{U}_α is a unimodular matrix, $\det \mathbf{U}_\alpha = 1$. Then,

$$\epsilon^{-1} = \frac{\tilde{\epsilon}}{\epsilon_A \epsilon_B}, \quad (\text{A.2})$$

where

$$\tilde{\epsilon} = \mathbf{R}(\epsilon_B \mathbf{U}_A^t (1 - B(\vec{r})) + \epsilon_A \mathbf{U}_B^t B(\vec{r})) \mathbf{R}^t \quad (\text{A.3})$$

is the response of the reciprocal system obtained by interchanging the scalar responses of A and B and transposing and rotating their orientation dependence (but without interchanging it). From here, we can follow all steps of section 2 from Eq. (32) to the main result (42) [6]. The only difference being the more complicated and somewhat artificial definition of the reciprocal system above. Some simplifications may be done when considering the symmetric nature of the matrix \mathbf{U}_α , and in the special case where $\mathbf{U}_A = \mathbf{U}_B$.

- [1] Joseph B. Keller. A theorem on the conductivity of a composite medium. *J. Math. Phys.*, 5:548, 1964.
- [2] A. M. Dykhne. Conductivity of a Two-dimensional Two-phase System. *Soviet Physics JETP*, 32:63, 1971.
- [3] Joseph B. Keller. Effective conductivity of periodic composites composed of two very unequal conductors. *Journal of Mathematical Physics*, 28(10):2516–2520, October 1987.
- [4] S. Mortola and S. Steffé. A two-dimensional homogenization problem. *Atti Accad. Naz. Lincei, Cl. Sci. Fis., Mat. Nat., Rend.*, 78:77, 1985.
- [5] Graeme W. Milton. Proof of a conjecture on the conductivity of checkerboards. *J. Math. Phys.*, 42:4873, 2001.
- [6] Kenneth S. Mendelson. A theorem on the effective conductivity of a two-dimensional heterogeneous medium. *J. Appl. Phys.*, 46(11):4740, 1975.
- [7] Kalman Schulgasser. On a phase interchange relationship for composite materials. *J. Math. Phys.*, 17:378, March 1976.
- [8] John E. Molyneux. Effective permittivity of a polycrystalline dielectric. *Journal of Mathematical Physics*, 11(4):1172–1184, 1970.
- [9] John Nevard and Joseph B. Keller. Reciprocal relations for effective conductivities of anisotropic media. *J. Math. Phys.*, 26:2761, November 1985.
- [10] K. Schulgasser. A reciprocal theorem in two-dimensional heat transfer and its implications. *International Communications in Heat and Mass Transfer*, 19(5):639–649, 1992. cited By 18.
- [11] Gerhard Kristensson and Niklas Wellander. Homogenization of the maxwell equations at fixed frequency. *SIAM Journal on Applied Mathematics*, 64(1):170–195, 2003.
- [12] Sebastian Guenneau, F Zolla, and A Nicolet. Homogenization of 3d finite photonic crystals with heterogeneous permittivity and permeability. *Waves in Random and Complex Media*, 17:653, October 2007.
- [13] P. Halevi, A. A. Krokhin, and J. Arriaga. Photonic Crystal Optics and Homogenization of 2d Periodic Composites. *Phys. Rev. Lett.*, 82(4):719–722, January 1999.
- [14] A.A.Krokhin, P. Halevi, and J.Arriaga. Long-wavelength limit (homogenization) for two-dimensional photonic crystal. *Phys. Rev. B*, 65:115208–1–115208–17, 2002.
- [15] P. Halevi and F. Pérez-Rodríguez. From photonic crystals (via homogenization) to metamaterials. In *Proc. SPIE: Complex Photonic Media*, volume 6320 of *SPIE Conference Series*. SPIE, 2006.
- [16] M. G. Silveirinha. Metamaterial homogenization approach with application to the characterization of microstructured composites with negative parameters. *Phys. Rev. B*, 75:115104, 2007.
- [17] W. L. Mochán and R. G. Barrera. Electromagnetic response of systems with spatial fluctuations. i. general formalism. *Phys. Rev. B*, 32:4984–4988, 1985.
- [18] W. L. Mochán and R. G. Barrera. Electromagnetic response of systems with spatial fluctuations. ii. applications. *Phys. Rev. B*, 32:4989–5001, 1985.
- [19] E. Cortes, W. Luis Mochán, B. S. Mendoza, and G. P. Ortiz. Optical properties of nanostructured metamaterials. *Phys. Stat. Sol. B*, 247(8):2102–2107, 2010.
- [20] W. Luis Mochán, Guillermo P. Ortiz, and Bernardo S. Mendoza. Efficient homogenization

- procedure for the calculation of optical properties of 3D nanostructured composites. *Opt. Express*, 18:22119–22127, 2010.
- [21] Guillermo Ortiz, Marina Inchaussandague, Diana Skigin, Ricardo Depine, and W Luis Mochán. Effective non-retarded method as a tool for the design of tunable nanoparticle composite absorbers. *Journal of Optics*, 16(10):105012, 2014.
- [22] Victor J. Toranzos, Guillermo P. Ortiz, W. Luis Mochán, and Jorge O. Zerbino. Optical and electrical properties of nanostructured metallic electrical contacts. *Mater. Res. Express*, 4:015026, 2017.
- [23] A. Sihvola. *Electromagnetic Mixing Formulas and Applications*, volume 47 of *IEE Electromagnetic Waves Series*. IEE, London, 1999.
- [24] Guillermo P. Ortiz, Brenda E. Martínez-Zérega, Bernardo S. Mendoza, and W.Luis Mochán. Effective optical response of metamaterials. *Phys. Rev. B*, 79:245132, 2009.
- [25] Bernardo S. Mendoza and W. Luis Mochán. Birefringent nanostructured metamaterials. *Phys. Rev. B*, 85:125418, 2012.
- [26] J. S. Pérez-Huerta, Guillermo P. Ortiz, Bernardo S. Mendoza, and W. Luis Mochán. Macroscopic optical response and photonic bands. *New J. Phys.*, 15(4):043037, 2013.
- [27] R. Haydock. The recursive solution of the Schrödinger equation. *Solid State Physics*, 35:215, 1980.
- [28] W. Luis Mochán, Guillermo Ortiz, Bernardo S. Mendoza, and José Samuel Pérez-Huerta. Photonic. Comprehensive Perl Archive Network (CPAN), 2016. Perl package for calculations on metamaterials and photonic structures.
- [29] William H. Press, Saul A. Teukolsky, William T. Vetterling, and Brian P. Flannery. *Numerical Recipes in C*. Cambridge University Press, New York, 2nd ed. edition, 1992.
- [30] Bernardo S. Mendoza and W. Luis Mochán. Tailored optical polarization in nano-structured metamaterials. *Phys. Rev. B*, 94:195137, 2016.